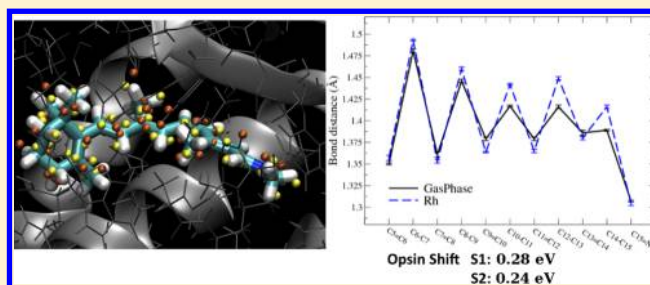# Protein Field Effect on the Dark State of 11-*cis* Retinal in Rhodopsin by Quantum Monte Carlo/Molecular Mechanics

Emanuele Coccia,[†] Daniele Varsano,[‡] and Leonardo Guidoni*,[†]

[†]Dipartimento di Scienze Fisiche e Chimiche, Università degli Studi dell'Aquila, via Vetoio, 67100, L'Aquila, Italy

[‡]Dipartimento di Fisica, "Sapienza" - Università di Roma, piazzale Aldo Moro 5, 00185, Rome, Italy

S *Supporting Information*

ABSTRACT: The accurate determination of the geometrical details of the dark state of 11-*cis* retinal in rhodopsin represents a fundamental step for the rationalization of the protein role in the optical spectral tuning in the vision mechanism. We have calculated geometries of the full retinal protonated Schiff base chromophore in the gas phase and in the protein environment using the correlated variational Monte Carlo method. The bond length alternation of the conjugated carbon chain of the chromophore in the gas phase shows a significant reduction when moving from the β-ionone

ring to the nitrogen, whereas, as expected, the protein environment reduces the electronic conjugation. The proposed dark state structure is fully compatible with solid-state NMR data reported by Carravetta et al. [*J. Am. Chem. Soc.* **2004**, *126*, 3948−3953]. TDDFT/B3LYP calculations on such geometries show a blue opsin shift of 0.28 and 0.24 eV induced by the protein for S_1 and S_2 states, consistently with literature spectroscopic data. The effect of the geometrical distortion alone is a red shift of 0.21 and 0.16 eV with respect to the optimized gas phase chromophore. Our results open new perspectives for the study of the properties of chromophores in their biological environment using correlated methods.
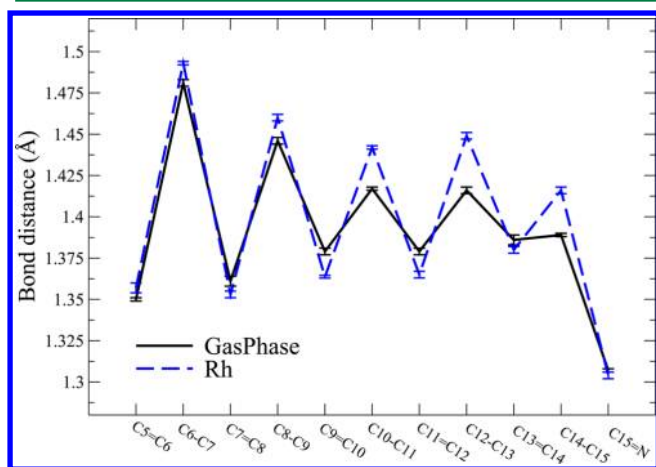
Rhodopsin is a light-detecting protein belonging to the family of G-protein-coupled receptors located in the rod cells of the retina of vertebrates, responsible for dim light vision.[1] Upon photon absorption, the embedded chromophore, the Retinal Protonated Schiff Base (**RPSB**, Figure 1) undergoes

Figure 1. The 11-*cis* Retinal Protonated Schiff Base (**RPSB**).

a very fast (∼200 fs) and efficient (quantum yield of ∼0.65) isomerization from the 11-*cis* to the all-*trans* conformer.[1,2] Femtosecond spectroscopy[3] and QM/MM molecular dynamics calculations[2,3] highlight the importance of the protein and of the hydrogen-out-of-plane (HOOP) motion[4] in the isomerization mechanism, involving an S_1/S_0 conical intersection[5] along the torsion of the central double bond C_{11}−C_{12}.

An accurate determination of the ground state structure of gas phase **RPSB** is a prerequisite to get a reliable starting point in the theoretical study of the isomerization mechanism and for the understanding of the role of the protein environment on the spectral tuning. Several key geometrical parameters such as the Bond Length Alternation (BLA) of the conjugated carbon chain (defined as the difference between single bond and double bond averages) and the dihedral angle $\varphi(C_5−C_6−C_7−C_8)$ involving the torsion of the β-ionone ring have been shown to be crucial in the tuning of the optical absorption.[6−8]

Because of the presence of an extended π-conjugated region in **RPSB**, the precise determination of the ground state geometrical parameters is still an open issue for theoretical chemistry. Within DFT, hybrid functionals like PBE0, B3LYP, and M06-2X[6,7,9,10] or long-range-corrected versions (CAM-B3LYP)[11] provide a ground state gas phase BLA ranging from 0.033 Å (B3LYP) to 0.053 Å (CAM-B3LYP). CASSCF calculations[12] give a larger average BLA of 0.101 Å, whereas the MP2 estimate[7,13] shows a decreased BLA, with a value of 0.044 Å.[7] In spite of these differences, all methods agree in asserting that the overall electrostatic and geometrical protein effect is to induce an evident reduction of the π-conjugation, leading to an increased BLA.[3,6,14,15]

Thanks to recent technical advances, Quantum Monte Carlo (QMC) methods[16] are becoming a suitable and correlated alternative in tackling the challenging task of calculating the electronic structure and the equilibrium geometries of molecular systems where electron correlation plays a crucial role, even in systems of biological interest.[17] In particular, the use of the Jastrow Antisymmetrized Geminal Power (JAGP) wave function[18] offers a compact and versatile variational ansatz

including both static and dynamical correlation, thanks to its multideterminant nature and to the Jastrow bosonic term.[19] In a preliminary work[20] on the retinal minimal model $C_5H_6NH_2^+$, we have demonstrated how compact JAGP wave functions can correctly reproduce ground state properties of this system such as isomerization energies, geometrical parameters, and dipole moments. The favorable scaling with the number N of electrons ($\propto N^{3,4}$) and the use of high performance computing facilities allows us to successfully apply QMC techniques to the study of many-electron problems and to afford similar calculations for the complete rhodopsin chromophore.

Adopting the computational procedure described in ref 20, we have used the Variational Monte Carlo (VMC) to fully optimize the ground state (S_0) geometry of **RPSB**, both in the gas phase (**GasPhase**) and embedded in the rhodopsin environment (**Rh**) exploiting a recently implemented Quantum Monte Carlo/Molecular Mechanics (QMC/MM) technique based on the QM/MM scheme in the CPMD code.[21] The QMC/MM calculations are based on the 1HZX crystallographic structure,[22] treating the full chromophore (as in Figure 1) at the VMC level. Our model comprises the full protein, water, and the cell membrane, simulated by a layer of n-octane molecules.[2] Glu181 is assumed to be negatively charged;[23a–c] His211, Asp83, and Glu122 are taken neutral as suggested by FTIR experiments.[23a,d] The MM part is described at the Amber/parm99 level for the protein and water molecules (TIP3P model), whereas we have used the OPLS force field for the n-octane.[2]

Three cavity waters (Wat2a, Wat2b, and Wat2c) have been located close to RPSB according to the more recent and resolved 1U19 structure.[24] A QM/MM annealing of the full system, at the BLYP level for the QM subsystem, has been performed: the overall relaxed structure has been used as a starting point for the QMC/MM calculations. Computational details of the VMC calculations and of the DFT annealing, together with a description of the QMC/MM machinery, are reported in the Supporting Information.

Figure 2 compares the BLA pattern for the **GasPhase** and **Rh** structures: the **GasPhase** structure is characterized by an average BLA of 0.059(3) Å, close to M06-2X (0.051 Å) and CAM-B3LYP (0.053 Å) results, while the average BLA assumes the value of 0.088(3) Å for **Rh** geometry. Moving from the β-ionone ring, one clearly sees a large similarity between the two structures up to the $C_8–C_9$ bond. The net effect of the environment is to increase the difference between single and double bond distances along the polyenic chain moving toward the nitrogen atom; in **GasPhase** no appreciable distinction is observed for $C_{13}=C_{14}$ and $C_{14}–C_{15}$ bonds, 1.386(3) Å and 1.389(1) Å, respectively. Such a remarkable nonhomogeneous BLA pattern for **GasPhase** can be explained in terms of delocalization along the polyenic chain of the positive charge, formally located on the nitrogen atom, consistently with ref 25. This is not the case for **Rh**, where the negatively charged Glu113 stabilizes the positive charge localizing it at the N terminus.
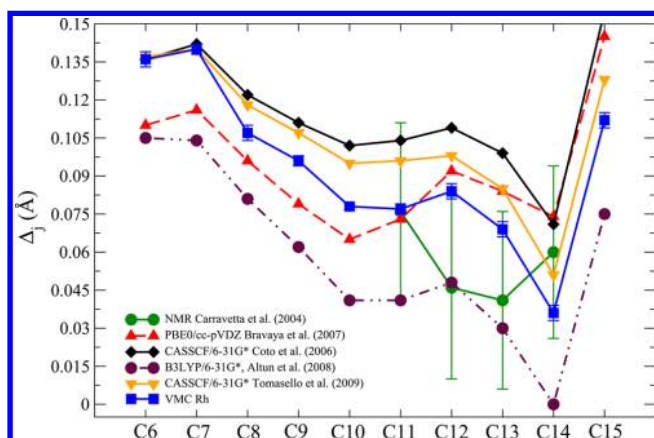
Our correlated VMC geometries are compared in Figure 3 with other available theoretical data. For what concerns the
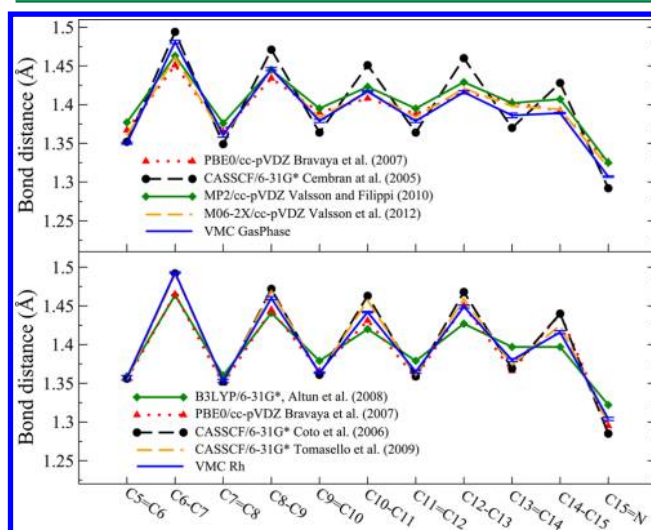
Figure 3. Comparison of the present VMC bond lengths with some selected, theoretical literature data for the **GasPhase** (upper panel) and **Rh** (lower panel) structures. Basis sets employed for the geometry optimization are also reported: for the PBE0 calculation,[6] aug-cc-pVDZ on oxygen atoms of the extended system has been used. The basis set for the VMC optimization is reported in Table 2 of the Supporting Information (SI).

isolated molecule (upper panel of Figure 3), the CASSCF structure seems to overestimate the BLA,[12] whereas DFT and MP2 calculations qualitatively describe a very similar reduction of BLA moving from the β-ionone ring to the nitrogen. In detail, the MP2 structure[7] is characterized by the same ratio between $C_{13}=C_{14}$ and $C_{14}–C_{15}$ bonds, and the DFT geometries, obtained with PBE0[6] and M06-2X[10] hybrid functionals, essentially coincide with our VMC findings in the central and N-terminus regions, $C_{13}=C_{14}$ bond excluded. Differences among the levels of theory[6,14,15,26] are softened with the introduction of the protein field in QM/MM calculations (lower panel of Figure 3) because of the partial suppression of the π-conjugation, with the exception of the B3LYP geometry,[26] characterized by a vanishing bond alternation in the N region; the QM subsystem in ref 6 also includes Glu113, Glu181, Ser186, and three water molecules.

A deeper insight on the details of the chromophore geometry embedded in protein can be achieved by defining a "local" BLA as the difference between two adjacent bond lengths R along the chain, $\Delta_j = |R_{j-1,j} - R_{j,j+1}|$. The VMC pattern is shown in Figure 4 together with four experimental points from solid state

Figure 2. BLA pattern of **RPSB** in the gas phase (solid black line) and within rhodopsin (dashed blue line), fully optimized at the variational Monte Carlo level.

Figure 4. Local BLA Δ_j (defined in the text) along the polyenic chain. NMR measurements from Carravetta et al.[25] with filled green circles and solid lines: comparison with VMC findings and other theoretical data.[6,14,15,26] The basis set for the VMC optimization is reported in Table 2 of the SI.

Table 1. TDDFT Excited States Energies and λ_{max} (eV and [nm]) of GasPhase, Dist, and Rh Structures, Calculated Using B3LYP, BLYP, and CAM-B3LYP Functionals[a]

	GasPhase	Dist	Rh
S_1 B3LYP	2.26 [549] $f = 0.95$	2.05 [605] $f = 0.66$	2.54 [488] $f = 1.00$
S_2 B3LYP	3.12 [397] $f = 0.80$	2.96 [419] $f = 0.76$	3.36 [369] $f = 0.52$
S_1 BLYP	1.97 [629] $f = 0.56$	1.73 [717] $f = 0.40$	2.17 [571] $f = 0.54$
S_2 BLYP	2.76 [449] $f = 0.88$	2.62 [473] $f = 0.66$	2.91 [426] $f = 0.81$
S_1 CAM-B3LYP	2.56 [484] $f = 1.49$	2.49 [498] $f = 1.19$	2.89 [429] $f = 1.44$
S_2 CAM-B3LYP	3.69 [336] $f = 0.38$	3.57 [347] $f = 0.38$	4.19 [296] $f = 0.24$
S_1 Exp refs 8,28,29	2.03−2.34 [530−610]		2.48(1) [500(2)]
S_2 Exp refs 28,29	3.18 [390]		3.27(1) [380(2)]

[a]The 6-311+G* basis set has been used for all the calculations. Oscillator strengths (f) are in italics.

NMR data reported in ref 25 and displayed as solid circles with error bars. All the VMC data are within the experimental error bars, distinct from the results obtained with other methods also reported in the same figure. In particular, CASSCF,[14,15] B3LYP,[26] and VMC data show a similar qualitative general trend from C_6 to C_{15}, with a minimum at C_{14}. The CASSCF and B3LYP Δ_j values are respectively larger and shorter than VMC ones, and the B3LYP[26] point at C14 is zero, at variance with the experimental and other theoretical findings. The qualitatively different PBE0[6] pattern could be explained in terms of the size of the QM subsystem.

An important aspect in the comparison among different QM approaches in Figures 3 and 4 is given by the details of the QM/MM setup and scheme employed in the calculations. A comparison between different QM methods (BLYP, B3LYP, QMC) within the same QM/MM scheme (same QM region size, QM/MM coupling, MM force field, protonation state of the residues, and annealing protocol) is reported and commented on in Figure 1 of the SI.

To investigate the optical properties of the VMC structures, we have calculated at the Time Dependent Density Functional Theory (TDDFT) level the vertical electronic excitations of the two first excited states S_1 and S_2,[27] which have been investigated by experiments both in the gas phase[8,28] and in the protein environment.[29] In Table 1, we report TDDFT results at the B3LYP, BLYP, and CAM-B3LYP levels on three different systems: the relaxed **GasPhase** structure, the gas phase distorted structure extracted by the QMC/MM geometry relaxation (**Dist**), and the relaxed QMC/MM structure embedded in the field of all protein atoms and of the three cavity water molecules (**Rh**). All the calculations have been performed using the Gaussian 09 package.[30]

The calculated **GasPhase** B3LYP excitation energies (S_1 = 2.26 eV, S_2 = 3.12 eV) are in a very good agreement with the experimental values.[8,28] The B3LYP S_1 energy also lies in the theoretical range, 2.20−2.36 eV, indicated by Valsson et al.[10] for several ground and excited state approaches. The S_1 energy calculated on the **GasPhase** structure is found in the "high-energy" region of the experimental band,[8] due to the partial break of conjugation on the β-ionone ring ($\varphi(C_5-C_6-C_7-C_8)$ = −42(1)°), in agreement with the findings reported by Rajput et al.[8] in the study of the effect of the torsion of the ring on the

absorption spectrum. It is important to remark that, besides the good agreement seen for S_2, TDDFT cannot properly describe the partial double-excitation character of such a state, found by CASPT2//CASSCF calculations.[5a,13,31−33]

In order to single out the effect of the environment on the optical properties of **RPSB**, we calculated TDDFT excitation energies on the **Dist** structure without including the external electrostatic field in the excited state calculations. The increasing of the BLA and the pretwisting of the dihedral angle observed in the structure strongly modify the optical properties inducing a red shift (with respect to the relaxed gas phase chromophore) of 0.21 eV for S_1 and 0.16 eV for S_2, at the B3LYP level, in qualitative agreement with previous theoretical data.[6,14,15,26]

Passing from the gas phase to the opsin environment, a blue shift in the absorption spectrum is found for both S_1 and S_2 states, corresponding to 0.28 and 0.24 eV, respectively, together with a reduction of the oscillator strength of the S_2 state.

BLYP excitation energies show a systematic red shift with respect to the B3LYP results and experiments. GGA approaches have already been seen to underestimate the low-lying excitation energies of the gas phase,[27a] protein embedded **RPSB** models,[26] and other biological chromophores,[34a] the red shift being ascribed due to the known failure of local and semilocal approximations in the description of polyenic chains.[34b]

Table 1 shows that an overall blue shift instead characterizes the CAM-B3LYP results. The S_1 and S_2 excitations coincide with the values reported by Rostov et al. on a CAM-B3LYP/6-31G(d) geometry.[27d] Moreover the observed shift does not strictly depend on the specific value of geometrical parameters of our VMC structures, as shown in Table 10 of the SI, where CAM-B3LYP energies are reported for several gas phase geometries obtained at different levels of theory.

In summary, in this Letter, we provide the ground state structures of the full rhodopsin chromophore in the gas phase and in its protein environment at a variational Monte Carlo level. The calculated **Rh** bond length differences have been found to be fully compatible within one standard deviation with the available NMR data. The ground and excited state energy components have been dissected in their distortion and protein

C

dx.doi.org/10.1021/ct3007502 | J. Chem. Theory Comput. XXXX, XXX, XXX−XXX

field contributions, indicating that the final opsin shift is the result of a red shift due to the geometrical distortion alone and a blue shift coming from the protein field. Coupling the correlated VMC structures with TDDFT/B3LYP calculations provides excitation energies very close to the experimental data.

Our results indicate that VMC is a powerful tool for the determination of accurate **RPSB** structures both in the gas phase and embedded in the protein environment. Beyond the results for rhodopsin biophysics, the present Letter demonstrates how quantum Monte Carlo calculations are mature enough to tackle large biological chromophores in their protein environment, opening new perspectives on accurate *ab initio* studies in photoreceptors.

■ ASSOCIATED CONTENT

Ⓢ Supporting Information

Details on the QMC/MM implementation and on the variational QMC wave function. Bond length alternation pattern in calculations. Kohn–Sham frontier orbitals and eigenvalues for **RPSB** in the gas phase and in rhodopsin. This material is available free of charge via the Internet at http://pubs.acs.org.

■ AUTHOR INFORMATION

Corresponding Author
*E-mail: leonardo.guidoni@univaq.it.

Notes
The authors declare no competing financial interest.

■ ACKNOWLEDGMENTS

■ REFERENCES

(1) Palczewski, K. *Annu. Rev. Biochem.* **2006**, *75*, 743–767.

(2) (a) Röhrig, U. F.; Guidoni, L.; Laio, A.; Frank, I.; Rothlisberger, U. *J. Am. Chem. Soc.* **2004**, *126*, 15328–15329. (b) Röhrig, U. F.; Guidoni, L.; Rothlisberger, U. *ChemPhysChem* **2005**, *6*, 1836–1847.

(3) (a) Frutos, L. M.; Andruniow, T.; Santoro, F.; Ferré, N.; Olivucci, M. *Proc. Natl. Acad. Sci. U. S. A.* **2007**, *104*, 7764–7769. (b) Polli, D.; Altoè, P.; Weingart, O.; Spillane, K. M.; Manzoni, C.; Brida, D.; Tomasello, G.; Orlandi, G.; Kukura, P.; Mathies, R. A.; Garavelli, M.; Cerullo, G. *Nature* **2010**, *467*, 440–442.

(4) (a) Schapiro, I.; Ryazantsev, M. N.; Frutos, L. M.; Ferré, N.; Olivucci, M. *J. Am. Chem. Soc.* **2011**, *133*, 3354–3364. (b) Weingart, O.; Altoè, P.; Stenta, M.; Bottoni, A.; Orlandi, G.; Garavelli., M. *Phys. Chem. Chem. Phys.* **2011**, *13*, 3645–3648.

(5) (a) Andruniow, T.; Ferré, N.; Olivucci, M. *Proc. Natl. Acad. Sci. U. S. A.* **2004**, *101*, 17908–17913. (b) Coto, P. B.; Sinicropi, A.; De Vico, L.; Ferré, N.; Olivucci, M. *Mol. Phys.* **2006**, *104*, 983–1008.

(6) Bravaya, K.; Bochenkova, A.; Granovski, A.; Nemukhin, A. *J. Am. Chem. Soc.* **2007**, *129*, 13035–13042.

(7) Valsson, O.; Filippi, C. *J. Chem. Theory Comput.* **2010**, *6*, 1275–1292.

(8) Rajput, J.; Rahbek, D. B.; Andersen, L. H.; Hirshfeld, A.; Sheves, M.; Altoè, P.; Orlandi, G.; Garavelli, M. *Angew. Chem.* **2010**, *122*, 1834–1837.

(9) Valsson, O.; Filippi, C. *J. Chem. Phys. Lett.* **2012**, *3*, 908–912.

(10) Valsson, O.; Angeli, C.; Filippi, C. *Phys. Chem. Chem. Phys.* **2012**, *14*, 11015–11020.

(11) Yanai, T.; Tew, D. P.; Handy, N. C. *Chem. Phys. Lett.* **2004**, *393*, 51–57.

(12) Cembran, A.; Gonzalez-Luque, R.; Altoè, P.; Merchan, M.; Bernardi, F.; Olivucci, M.; Garavelli, M. *J. Phys. Chem. A* **2005**, *109*, 6597–6605.

(13) Sekharan, S.; Weingart, O.; Buss, V. *Biophys. J.* **2006**, *91*, L07–L09.

(14) Tomasello, G.; Olaso-Gonzalez, G.; Altoè, P.; Stenta, M.; Serrano-Andres, L.; Merchan, M.; Orlandi, G.; Bottoni, A.; Garavelli, M. *J. Am. Chem. Soc.* **2009**, *131*, 3948–3953.

(15) Coto, P. B.; Strambi, A.; Ferré, N.; Olivucci, M. *Proc. Natl. Acad. Sci. U. S. A.* **2006**, *103*, 17154–17159.

(16) Foulkes, W. M. C.; Mitas, L.; Needs, R. J.; Rajagopal, G. *Rev. Mod. Phys.* **2001**, *73*, 33–83.

(17) Filippi, C.; Buda, F.; Guidoni, F.; Sinicropi, A. *J. Comput. Chem. Theory* **2012**, *8*, 112.

(18) (a) Casula, M.; Sorella, S. *J. Chem. Phys.* **2003**, *119*, 6500–6511. (b) Casula, M.; Attaccalite, C.; Sorella, S. *J. Chem. Phys.* **2004**, *121*, 7110–7126. (c) Casula, M.; Filippi, C.; Sorella, S. *Phys. Rev. Lett.* **2005**, *95*, 100201-1–4. (d) Sorella, S.; Casula, M.; Rocca, D. *J. Chem. Phys.* **2007**, *127*, 14105–14116. (e) Casula, M.; Moroni, S.; Sorella, S.; Filippi, C. *J. Chem. Phys.* **2010**, *132*, 154113–154121. (f) Sorella, S.; Capriotti, L. *J. Chem. Phys.* **2010**, *133*, 234111–234120.

(19) (a) Barborini, M.; Sorella, S.; Guidoni, L. *J. Chem. Theory Comput.* **2012**, *8*, 1260–1269. (b) Coccia, E.; Chernomor, O.; Barborini, M.; Sorella, S.; Guidoni, L. *J. Chem. Theory Comput.* **2012**, *8*, 1952–1962.

(20) Coccia, E.; Guidoni, L. *J. Comput. Chem.* **2012**, *33*, 2332–2339.

(21) *CPMD*; IBM Corp.: Armonk, NY, 1990–2008; MPI für Festkörperforschung Stuttgart: Stuttgart, Germany, 1997–2001. http://www.cpmd.org (accessed date 19 November, 2012).

(22) Teller, D. C.; Okada, T.; Behnke, C. A.; Palczewski, K.; Stenkamp, R. E. *Biochemistry* **2001**, *40*, 7761–7772.

(23) (a) Lüdeke, S.; Beck, M.; Yan, E. C. Y.; Sakmar, T. P.; Siebert, F.; Vogel, R. *J. Mol. Biol.* **2005**, *353*, 345. (b) Röhrig, U. F.; Guidoni, L.; Rothlisberger, U. *Biochemistry* **2002**, *41*, 10799–10809. (c) Sanberg, M. N.; Amora, T. L.; Ramos, L. S.; Chen, M.-S.; Knox, B. E.; Birge, R. R. *J. Am. Chem. Soc.* **2011**, *133*, 2808. (d) Fahmy, K.; Jager, F.; Beck, M.; Zvyaga, T. A.; Sakmar, T. P.; Siebert, F. *Proc. Natl. Acad. Sci. U. S. A.* **1993**, *90*, 10206–10210.

(24) Okada, T.; Minoru, S.; Bondard, A.; Elstnerf, M.; Entelc, P.; Buss, V. *J. Mol. Biol.* **2004**, *342*, 571–583.

(25) Carravetta, M.; Zhao, X.; Johannessen, O. G.; Lai, W. C.; Verhoeven, M. A.; Bovee-Geurts, P. H. M.; Verdegem, P. J. E.; Kiihne, S.; Luthman, H.; de Groot, H. J. M.; deGrip, W. J.; Lugtenburg, J.; Levitt, M. H. *J. Am. Chem. Soc.* **2004**, *126*, 3948–3953.

(26) Altun, A.; Yokoyama, S.; Morokuma, K. *J. Phys. Chem. B* **2008**, *112*, 6814–6827.

(27) (a) Wanko, M.; Garavelli, M.; Bernardi, F.; Niehaus, T. A.; Frauenheim, T.; Elstner, M. *J. Chem. Phys.* **2004**, *120*, 1674–1692. (b) Send, R.; Sundholm, D. *J. Phys. Chem. A* **2007**, *111*, 8766–8773. (c) Zaari, R. R.; Wong, S. Y. Y. *Chem. Phys. Lett.* **2008**, *469*, 224–228. (d) Rostov, I. V.; Amos, R. D.; Kobayashi, R.; Scalmani, G.; Frisch, M. J. *J. Phys. Chem. B* **2010**, *114*, 5547–5555. (e) Kaila, V. R. I.; Send, R.; Sundholm, D. *J. Phys. Chem. A* **2012**, *116*, 2249–2258.

(28) (a) Andersen, L. H.; Nielsen, I. B.; Kristensen, M. B.; El Ghazaly, M. O. A.; Haacke, S.; Brønsted Nielsen, M.; Åxman Petersen, M. *J. Am. Chem. Soc.* **2005**, *127*, 12347–12350. (b) Nielsen, I. B.; Lammich, L.; Andersen, L. H. *Phys. Rev. Lett.* **2006**, *96*, 18304-1–4.

(29) (a) Vikram, R. R.; Oprian, D. D. *Annu. Rev. Biophys. Biomol. Struct.* **1996**, *25*, 287–314. (b) Sakmar, T. P.; Menon, S. T.; Marin, E. P.; Award, E. S. *Annu. Rev. Biophys. Biomol. Struct.* **2002**, *31*, 443–484. (c) Filipek, S.; Stenkamp, R. E.; Teller, D. C.; Palczewski, K. *Annu. Rev. Physiol.* **2003**, *65*, 851–879.

(30) Frisch, M. J.; Trucks, G. W.; Schlegel, H. B.; Scuseria, G. E.; Robb, M. A.; Cheeseman, J. R.; Scalmani, G.; Barone, V.; Mennucci,

B.; Petersson, G. A.; Nakatsuji, H.; Caricato, M.; Li, X.; Hratchian, H. P.; Izmaylov, A. F.; Bloino, J.; Zheng, G.; Sonnenberg, J. L.; Hada, M.; Ehara, M.; Toyota, K.; Fukuda, R.; Hasegawa, J.; Ishida, M.; Nakajima, T.; Honda, Y.; Kitao., O.; Nakai, H.; Vreven, T.; Montgomery, J. A., Jr.; Peralta, J. E.; Ogliaro, F.; Bearpark, M.; Heyd, J. J.; Brothers, E.; Kudin, K. N.; Staroverov, V. N.; Kobayashi, R.; Normand, J.; Raghavachari, K.; Rendell, A.; Burant, J. C.; Iyengar, S. S.; Tomasi, J.; Cossi, M.; Rega, N.; Millam, J. M.; Klene, M.; Knox, J. E.; Cross, J. B.; Bakken, V.; Adamo, C.; Jaramillo, J.; Gomperts, R.; Stratmann, R. E.; Yazyev, O.; Austin, A. J.; Cammi, R.; Pomelli, C.; Ochterski, J. W.; Martin, R. L.; Morokuma, K.; Zakrzewski, V. G.; Voth, G. A.; Salvador, P.; Dannenberg, J. J.; Dapprich, S.; Daniels, A. D.; Farkas, O.; Foresman, J. B.; Ortiz, J. V.; Cioslowski, J.; Fox, D. J. *Gaussian 09*, Revision A.1; Gaussian, Inc.: Wallingford, CT, 2009.

(31) Hufen, J.; Sugihara, M.; Buss, V. *J. Phys. Chem B* **2004**, *108*, 20419−20426.

(32) Elliott, P.; Goldson, S.; Canahui, C.; Maitra, N. T. *Chem. Phys.* **2011**, *391*, 110−119.

(33) Sekharan, S.; Sugihara, M.; Weingart, O.; Okada, T.; Buss, V. *J. Am. Chem. Soc.* **2007**, *129*, 1052−1054.

(34) (a) Muguruza Gonzàlez, E.; Guidoni, L.; Molteni, C. *Phys. Chem. Chem. Phys.* **2009**, *11*, 4556−4563. (b) Varsano, D.; Marini, A.; Rubio, A. *Phys. Rev. Lett.* **2008**, *101*, 133002-1−4.